J. Mech. Phys. Solids Vol. 36, No. 2, pp. 189–214, 1988.
Printed in Great Britain.

0022–5096/88 $3.00+0.00


# CRACK TIP SINGULAR FIELDS IN DUCTILE CRYSTALS WITH TAYLOR POWER-LAW HARDENING. I: ANTI-PLANE SHEAR

JAMES R. RICE and MARYAM SAEEDVAFA

Division of Applied Sciences, Harvard University, Cambridge, Massachusetts 02138, U.S.A.

(*Received* 2 *June* 1987)

ABSTRACT

ASYMPTOTIC singular solutions of the HRR type are presented for anti-plane shear cracks in ductile crystals. These are assumed to undergo Taylor hardening with a power-law relation between stress and strain at sufficiently large strain. Results are given for several crack orientations in fcc and bcc crystals. The near-tip region divides into angular sectors which are the maps of successive flat segments and vertices on the yield locus. Analysis is simplified by use of new general integrals of crack tip singular fields of the HRR type. It is conjectured that the single crystal HRR fields are dominant only over part of the plastic region immediately adjacent to the crack tip, even at small scale yielding, and that their domain of validity vanishes as the perfectly plastic limit is approached. This follows from the fact that while in the perfectly plastic limit the HRR stress states approach the correct discontinuous distributions of the complete elastic–ideally plastic solutions for crystals (RICE and NIKOLIC, *J. Mech. Phys. Solids* **33**, 595 (1985)), the HRR displacement fields in that limit remain continuous. Instead, the complete elastic–ideally plastic solutions have discontinuous displacements along planar plastic regions emanating from the tip in otherwise elastically stressed material. The approach of the HRR stress fields to their discontinuous limiting distributions is illustrated in graphical plots of results. A case examined here of a fcc crystal with a crack along a slip plane is shown to lead to a discontinuous near-tip stress state even in the hardening regime.

Through another limiting process, the asymptotic solution for the near-tip field for an isotropic material is also derived from the present single crystal framework.

## INTRODUCTION

THE PRESENT article analyzes singular near-tip stress and deformation fields for stationary anti-plane shear (mode III) loaded cracks in strain hardening ductile crystals. It is assumed that the crystals deform by shear on a set of allowable slip systems according to the Schmid rule. That is, plastic flow occurs on a given system once the resolved shear stress on that system reaches a critical value. In addition, the critical shear strengths are assumed to obey Taylor hardening (all systems harden equally) with a power-law relation between stress and strain at sufficiently large strain. Thus, the yield surfaces in stress space, being the inner envelope of the planar yield surfaces for individual slip systems, reduce to self-similar polygons in the two-dimensional anti-plane shear stress plane. The yield surface is a fixed polygon in the space of the ratio of the stresses to the critical shear strength.

In the near-tip field, it is anticipated that the elastic strains are relatively small and ignorable. Hence the entire strain vector can be identified with the plastic strains.

Since the above constitutive description is compatible with the maximum plastic work inequality, and hence involves an associated flow rule, the strain vector will be normal to the yield surface along flat segments and within the fan of limiting normals at a vertex.

Continuity of stress and displacements is anticipated through the whole field. In some cases this continuity condition is satisfied only in the generalized form of a vanishing sector. For mode III, the equations of equilibrium, together with stress-strain relations consistent with the above description and strain-displacement gradient relations, lead to simple non-linear equations which can be solved analytically.

The polygonality of the yield surface results in two different types of solution referring to stress states corresponding to either a flat segment or a vertex point of the surface. As the yield surface is traversed, the angular range near the tip will be divided into sectors corresponding to these possible stress states.

Previous work on anti-plane shear loaded cracks in ductile crystals was done by RICE and NIKOLIC (1985), where complete elastic–plastic analysis was carried out for ideally plastic crystals with stationary and moving cracks. Their analysis for the stationary case included a full-field solution as well as an asymptotic near-tip analysis. The equations of the latter, taken alone, did not yield a unique strain field. In this paper, their near-tip field solution has been expanded to include power-law hardening material. It is to be expected that the current results will converge to their results in the non-hardening limit, but may show a different type of strain field within the family of allowable fields in their asymptotic analysis.

Mode III solutions for isotropic power-law hardening material have been known for several years. RICE (1967) discussed a method for deriving the solution by formulating the equations for the physical coordinates in terms of strains. The isotropic yield surface consists of a simple circle in the space of stresses. Since a circle, in the limit, is an infinite-sided polygon, a direct solution for the isotropic mode III field may be derived as the limit of the solution here for a single crystal polygonal yield surface, and such results are given here.

## MATHEMATICAL FORMULATION

A Cartesian coordinate system fixed with the crack tip is used, as shown in Fig. 1. Conventional index notation is utilized where repeated indices imply summation. Greek indices $\alpha$, $\beta$, . . . , range over 1 and 2, while Latin indices $i$, $j$, . . . , have the values of 1, 2 and 3. It is assumed that the crack and crystal orientations, and the method of loading, are such that anti-plane shear is a possible deformation state. That is, displacement $u_3 = u_3(x_1, x_2)$. Then, the yield surface reduces to a polygon, as discussed above, in a plane whose axes are the anti-plane shear stresses, $\sigma_{13}$ and $\sigma_{23}$.

The polar coordinates $r$ and $\theta$ have associated unit vectors $\mathbf{e}$ and $\mathbf{h}$ which are in the radial and angular directions respectively. Also,

$$\partial r/\partial x_\alpha = e_\alpha, \quad \partial\theta/\partial x_\alpha = h_\alpha/r, \tag{1}$$

will govern the transformation to polar coordinates. Coordinate rotations will be used

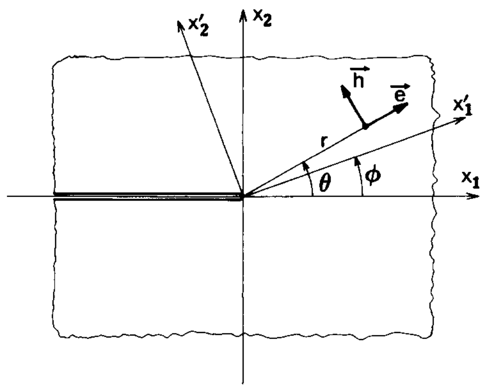


FIG. 1. Coordinate system used.

to simplify the derivation. For a counter-clockwise rotation by an angle $\phi$, as in Fig. 1, vector transformation is governed by the rule

$$x_1 + \mathrm{i}x_2 = \mathrm{e}^{i\phi}(x'_1 + \mathrm{i}x'_2), \tag{2}$$

where $\mathrm{i} = \sqrt{-1}$, which also applies to $\sigma_{31} + \mathrm{i}\sigma_{32}$, etc.

For mode III, the single non-trivial equation of equilibrium, in terms of the only non-zero components of stress, is

$$\partial\sigma_{\alpha 3}/\partial x_\alpha = \partial\sigma_{13}/\partial x_1 + \partial\sigma_{23}/\partial x_2 = 0, \tag{3}$$

whereas strains are given by

$$2\varepsilon_{3\alpha} = \gamma_{3\alpha} = \partial u_3/\partial x_\alpha. \tag{4}$$

An effective shear strain $\gamma$ for the Taylor hardening model may be defined by

$$\mathrm{d}\gamma = \sum_k \mathrm{d}\gamma^k, \tag{5}$$

where $\mathrm{d}\gamma^k$ is the plastic shear strain increment on the $k$th slip system, always taken positive in the direction of slip, and the sum is taken over all active slip systems. Let $\tau$ be the critical resolved shear stress which, due to the Taylor hardening model, is the same for all possible slip systems. Then,

$$\begin{aligned} \mathrm{d}\varepsilon_{ij} &= \sum_k \mu_{ij}^k\, \mathrm{d}\gamma^k, \\ \tau = \tau^k &= \mu_{ij}^k \sigma_{ij}, \end{aligned} \tag{6}$$

where $\mu_{ij}^k$ is the Schmid factor defined as $\mu_{ij}^k = (n_i^k s_j^k + n_j^k s_i^k)/2$ (no sum here on $k$). Here $\mathbf{n}$ is the unit outward normal to the slip plane and $\mathbf{s}$ is the unit vector in the slip direction. Thus,

$$\tau\,\mathrm{d}\gamma = \tau \sum_k \mathrm{d}\gamma^k = \sum_k \sigma_{ij}\mu_{ij}^k\, \mathrm{d}\gamma^k = \sigma_{ij}\, \mathrm{d}\varepsilon_{ij}. \tag{7}$$

Then for proportional stressing and straining (as with the HRR singular fields to be discussed later)

$$\gamma = \sum_k \gamma^k, \tag{8}$$

$$\tau\gamma = \sigma_{ij}\varepsilon_{ij}. \tag{9}$$

The material is assumed to be strain-hardening following a power-law of the form

$$\gamma = a\tau^n, \tag{10}$$

where $a$ is the hardening constant and $n$ is the hardening exponent; $n \to \infty$ is the perfectly plastic limit.

The plastic material described responds identically, under proportional stressing, as a non-linear elastic material of energy density

$$W = \int_0^{\varepsilon_{mn}} \sigma_{ij}\,\mathrm{d}\varepsilon_{ji} = [n/(n+1)]\sigma_{ij}\varepsilon_{ji} = [n/(n+1)]\tau\gamma. \tag{11}$$

This means that a $J$-integral can then be associated with the HRR singular field and some general integrals of elastic crack tip singular fields (RICE, 1988) may be utilized. Rather than explicitly identifying $W$ as a (symmetric) function of the $\varepsilon_{ij}$, in terms of which $\sigma_{ij} = \partial W/\partial\varepsilon_{ji}$, it is simpler to work with the complementary energy density $\Omega = \sigma_{ij}\varepsilon_{ji} - W$. Regarding $\Omega$ as a function of the $\sigma_{ij}$, then $\varepsilon_{ij} = \partial\Omega/\partial\sigma_{ji}$. A function $\Omega$ compatible with the Taylor hardening model will result when level surfaces of $\Omega$, for the non-linear elastic solid, are coincident with yield surfaces of the plastic solid corresponding to appropriately constant values of $\tau$. Thus motivated, it is evident that

$$\Omega = a\tau^{(n+1)}/(n+1) \tag{12}$$

where, in this expression, $\tau$ = maximum on $k$ of $\mu^k_{ij}\sigma_{ij}$, gives the proper function of stress. This results in an $\varepsilon_{ij}$ which is normal to a flat segment of the yield (or complementary energy) surface, and properly indeterminate within the cone of limiting normals at a vertex. For example, if a stressing path along which systems "1" and "2" are equally stressed, and all others are less stressed, is considered, then $\partial\tau/\partial\sigma_{ij}$ is consistently interpreted as $m\mu^1_{ij} + (1-m)\mu^2_{ij}$ for arbitrary $m$ in the interval $0 \leqslant m \leqslant 1$. Thus this $\Omega$ results, by (10), in $\varepsilon_{ij} = m\gamma\mu^1_{ij} + (1-m)\gamma\mu^2_{ij}$, which evidently agrees with the plastic relation of (5) and (6).

For power-law hardening plastic material, in which proportional stress states of a type indistinguishable from those for the analogous non-linear elastic solid are possible, the stress and displacement gradients near the crack tip must be such that the $J$-integral is path-independent and hence, when evaluated over a circular path surrounding the tip, is independent of $r$. As discussed by HUTCHINSON (1968) and RICE and ROSENGREN (1968), this type of field (referred to as HRR) must therefore have singular near-tip stresses, strains and displacements of the form

$$\begin{aligned} \sigma_{ij} &= r^{-1/(n+1)}\hat{\sigma}_{ij}(\theta), \\ \varepsilon_{ij} &= r^{-n/(n+1)}\hat{\varepsilon}_{ij}(\theta), \\ u_i &= r^{+1/(n+1)}\hat{u}_i(\theta), \end{aligned} \tag{13}$$

if singular solutions of the type $u \sim r^\lambda$ exist as $r \to 0$.

## General Integrals of HRR Singular Fields

Rice (1988) derived two general integrals of all crack tip singular fields in non-linear elastic (or elastic–plastic, under conditions noted above) materials for which products of the form $r\sigma_{ij}\partial u_j/\partial x_k$ have a finite limit as $r \to 0$. This evidently includes the HRR singular fields of (13). His results follow from the fact that in homogeneous material the integrals $J_\beta = \oint N_\alpha E_{\alpha\beta}\,ds = 0$ on all closed contours (not surrounding the crack tip), where $N_\alpha$ is the outer normal and $E_{\alpha\beta}$ is the Eshelby tensor

$$E_{\alpha\beta} = W\delta_{\alpha\beta} - \sigma_{\alpha j}\partial u_j/\partial x_\beta. \tag{14}$$

Thus, $\partial E_{\alpha\beta}/\partial x_\alpha = 0$, whereas components of $E_{\alpha\beta}$ have singularities of the type $F_{\alpha\beta}(\theta)/r$ at the crack tip. From these considerations, he showed that the singular field must satisfy

$$rh_\alpha E_{\alpha\beta} = r[Wh_\beta - h_\alpha\sigma_{\alpha j}\partial u_j/\partial x_\beta] = -C_\beta \text{ (constants)}, \quad \beta = 1, 2, \tag{15}$$

in the limit $r \to 0$ (or for all $r$, if just the singular field is considered as in (13)). He also noted that crack free surface boundary conditions, $h_\alpha\sigma_{\alpha j} = 0$, on the walls of the crack (where $h_1 = 0$), require that $C_1 = 0$. Further, since $h_2 = -1$ and $W \geqslant 0$ along the crack walls, $C_2 \geqslant 0$.

It may be noted that for HRR fields,

$$r\partial u_j/\partial x_\beta e_\beta = r\partial u_j/\partial r = u_j/(n+1). \tag{16}$$

Thus, by multiplying the pair of integrals (15) with $e_\beta$, one has

$$rh_\alpha\sigma_{\alpha j}\partial u_j/\partial x_\beta e_\beta = C_\beta e_\beta, \tag{17}$$

which can be rewritten as

$$h_\alpha\sigma_{\alpha j}u_j = (n+1)C_2 e_2 = (n+1)C_2\sin\theta. \tag{18}$$

Also, by multiplying (15) with $h_\beta$,

$$rW - h_\alpha\sigma_{\alpha j}\partial u_j/\partial\theta = -C_\beta h_\beta = -C_2\cos\theta, \tag{19}$$

since $h_\beta h_\beta = 1$ and $rh_\beta\partial/\partial x_\beta = \partial/\partial\theta$.

Equations (18) and (19) are alternate forms for the two general integrals of (15). These equations apply to all power-law hardening materials, and all loading modes or mixed mode combinations, for which HRR singular fields exist. In analysis of such HRR fields, (18) and (19) may be used in lieu of two of what would otherwise be the set of independent governing equations (stress equilibrium, strain-displacement compatibility, and stress-strain relations) for the field. For example, Rice (1988) showed how (18) and (19), together with stress–strain relations for the isotropic power hardening material in mode III, provide a complete solution for the HRR singular field in that case. For mode III, (18) reduces to

$$h_\alpha\sigma_{\alpha 3}u_3 = \sigma_{\theta 3}u_3 = (n+1)C_2\sin\theta. \tag{20}$$

Equation (19) can be derived rather easily from (18), by differentiation with respect

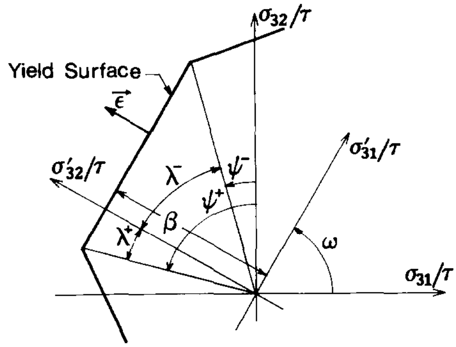


FIG. 2. Notation used for the flat segment of the yield surface.

to $\theta$, when one makes use of the stress equilibrium equations for stress states of HRR type, i.e., when one notes that $\partial\sigma_{\alpha j}/\partial x_\alpha = 0$ imply

$$h_\alpha \partial\sigma_{\alpha j}/\partial\theta - e_\alpha\sigma_{\alpha j}/(n+1) = 0, \tag{21}$$

and uses the special form of $rW$,

$$rW = [n/(n+1)]r\sigma_{ij}\partial u_j/\partial x_i = [n/(n+1)]\,[h_\alpha\sigma_{\alpha j}\partial u_j/\partial\theta + e_\alpha\sigma_{\alpha j}u_j/(n+1)], \tag{22}$$

for HRR fields. However, a simple direct derivation (other than that outlined here) for either of (18) or (19) singly has not been found.

Effective application of (18) is shown in what follows. It is useful because the HRR solutions for single crystals are developed sector by sector, and the constants $C_1$ $(=0)$ and $C_2$ must be the same for all sectors. Thus (18) is greatly helpful in assembling the sectors and it allows the definition of the whole field in terms of a single unknown constant $C_2$. This simplifies the calculations of single crystal HRR fields significantly in mode III and yet more so in mode I (SAEEDVAFA and RICE, work in progress).

## FLAT SECTORS

It is assumed that the whole angular range about the crack tip responds plastically. Consider an angular sector of points near the tip which correspond to a particular flat segment of the yield surface. Note that since the HRR field (13) involves ratios of stresses to one another that are independent of $r$, each ray $\theta =$ constant of the sector corresponds to a particular point of a fixed flat segment in the plane of Fig. 2, with axes $\sigma_{31}/\tau$ and $\sigma_{32}/\tau$. The normality rule requires the strain vector to be perpendicular to that segment as shown in Fig. 2. Thus, rotating the axes by an angle $\omega$ such that the $\sigma'_{32}/\tau$ axis is perpendicular to the segment (which causes the same orientation for the $x'_2$ axis) yields

$$\gamma'_{31} = \frac{\partial u_3}{\partial x'_1} = 0. \tag{23}$$

Thus

$$u_3 = u = u(x'_2). \tag{24}$$

For HRR fields $u$ varies as $r^{1/(n+1)}$ and since $x'_2 = r\sin(\theta-\omega)$, (24) leads to

$$u = A_1 x'_2 |x'_2|^{-n/(n+1)}, \tag{25}$$

$$\gamma'_{32} = \frac{\partial u}{\partial x'_2} = \frac{A_1}{(n+1)}|x'_2|^{-n/(n+1)}, \tag{26}$$

where $A_1 \geqslant 0$ is a constant. For the flat segment of the yield surface $\sigma'_{32}/\tau$ has a constant value of $\beta$. The constant $\beta = 1$ when, for a slip system stressed to yield in correspondence with the flat segment considered, one of **n** and **s** is in the $x_3$ direction and the other in the $x_1$–$x_2$ plane. Otherwise, $\beta$ may exceed 1. Observe that by (9) $\tau\gamma = 2\sigma_{3\alpha}\varepsilon_{3\alpha} = \sigma_{3\alpha}\gamma_{3\alpha} = \sigma'_{3\alpha}\gamma'_{3\alpha} = \sigma'_{32}\gamma'_{32} = \beta\tau\gamma'_{32}$. Thus, $\gamma = \beta\gamma'_{32}$ which implies $\tau = (\beta\gamma'_{32}/a)^{1/n}$ by (10) and therefore

$$\sigma'_{32} = \beta\left[\frac{\beta A_1}{(n+1)a}\right]^{1/n}|x'_2|^{-1/(n+1)}. \tag{27}$$

Using (3) transformed into this new coordinate system and integrated with respect to $x'_1$, yields

$$\sigma'_{31} = \frac{\beta}{(n+1)}\left[\frac{\beta A_1}{(n+1)a}\right]^{1/n}|x'_2|^{-1/(n+1)-2}x'_2x'_1 + f(x'_2). \tag{28}$$

For HRR fields, stresses vary as $r^{-1/(n+1)}$. Therefore, since $x'_2 = r\sin(\theta-\omega)$, the last term in (28) must be a constant times $|x'_2|^{-1/(n+1)}$, or

$$\sigma'_{31} = \frac{\beta}{(n+1)}\left[\frac{\beta A_1}{(n+1)a}\right]^{1/n}|x'_2|^{-1/(n+1)}\left[\frac{x'_1}{x'_2} + A_2\right]. \tag{29}$$

Now using (20) in the transformed coordinate system, $A_1$ and $A_2$ can be calculated as

$$A_1 = \frac{(n+1)}{\beta}\left[\frac{(n+1)}{n}C_2\frac{|x'_2|}{x'_2}\sin\omega\right]^{n/(n+1)}a^{1/(n+1)}, \tag{30}$$

$$A_2 = -n\cot\omega. \tag{31}$$

Note that in this sector $x'_2$ cannot change sign or the stresses will become infinite along the line $x'_2 = 0$. Also, from (30), the sign of $x'_2$ within the sector must agree with that of $\sin\omega$.

*Sector Limits.* Since the flat sector of the yield locus adjoins two vertices, the range of applicability of (23) through (31) is confined to

$$\tan(-\lambda^+) \leqslant \frac{\sigma'_{31}}{\sigma'_{32}} \leqslant \tan\lambda^-, \tag{32}$$

where $\lambda^-$ and $\lambda^+$ are defined in Fig. 2 as $\lambda^- = \omega - \psi^-$ and $\lambda^+ \leqslant \psi^+ - \omega$. Thus, using (27), (29) and (31) leads to

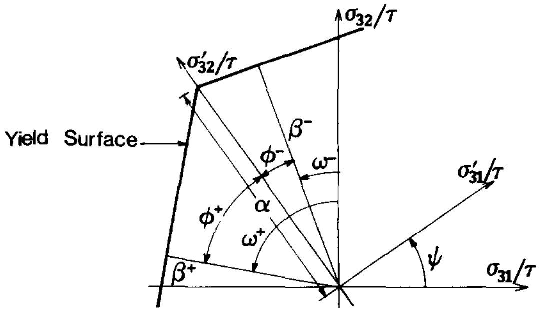


FIG. 3. Notation used for the vertex point of the yield surface. Here $\alpha = \beta^+/\cos(\omega-\psi^+) = \beta^-/\cos(\omega-\psi^-)$.

$$(n+1)\tan(\omega-\psi^-)+n\cot\omega \leqslant \cot(\theta-\omega) \leqslant (n+1)\tan(\omega-\psi^+)+n\cot\omega. \quad (33)$$

Simplifying (33), it is obtained that the flat sector ends (or starts) when $\theta = \theta^{F+}$ (or $\theta^{F-}$), satisfying

$$\tan\theta^F = (n+1)\frac{1+\tan(\omega-\psi)\tan\omega}{(n+1)\tan(\omega-\psi)+n\cot\omega-\tan\omega} \quad (34)$$

with $\psi = \psi^+$ (or $\psi^-$).

## VERTEX SECTORS

For the angular range near the tip which corresponds to a stress state at a vertex of the yield surface, the ratio of stresses to the effective stress $\tau$ will remain constant. The strain vector changes its orientation continuously in the range bounded by the two normals to the flat segments which meet at the vertex. Using a coordinate system where the $\sigma'_{32}/\tau$ axis passes through the vertex, that is by rotating the axes by an angle $\psi$, as shown in Fig. 3, yields

$$\sigma'_{31} = 0. \quad (35)$$

Integrating (3) with respect to $x'_2$ after substituting (35), and recognizing the special functional form of stress in HRR fields, results in

$$\sigma'_{32} = B_1|x'_1|^{-1/(n+1)}, \quad (36)$$

with $B_1 \geqslant 0$. Note that as shown in Fig. 3, $\sigma'_{32} = \alpha\tau$ where $\alpha$ can be defined in terms of the constant $\beta$ of either of the neighboring flat sectors as $\alpha = \beta/\cos(\omega-\psi)$. Similar to the calculations for the flat sector, using (9) leads to $\tau\gamma = \sigma_{3\alpha}\gamma_{3\alpha} = \sigma'_{32}\gamma'_{32} = \alpha\tau\gamma'_{32}$ and thus applying (10) results in $\gamma'_{32} = \gamma/\alpha = a(\sigma'_{32}/\alpha)^n/\alpha$, or

$$\gamma'_{32} = \frac{\partial u}{\partial x'_2} = \frac{a}{\alpha}\left(\frac{B_1}{\alpha}\right)^n |x'_1|^{-n/(n+1)}. \quad (37)$$

This is integrated to obtain $u$ and hence $\gamma'_{31}$ as

$$u = \frac{a}{\alpha}\left(\frac{B_1}{\alpha}\right)^n |x_1'|^{1/(n+1)} \frac{x_1'}{|x_1'|}\left(\frac{x_2'}{x_1'} + B_2\right), \tag{38}$$

$$\gamma_{31}' = \frac{\partial u}{\partial x_1'} = \frac{a}{\alpha(n+1)}\left(\frac{B_1}{\alpha}\right)^n |x_1'|^{-n/(n+1)}\left(-n\frac{x_2'}{x_1'} + B_2\right). \tag{39}$$

Now application of (20) leads to

$$B_1 = \alpha\left[(n+1)\frac{C_2}{a}\cos\psi\frac{x_1'}{|x_1'|}\right]^{1/(n+1)}, \tag{40}$$

$$B_2 = \tan\psi. \tag{41}$$

Here $x_1'$ must have the same sign through the whole domain of validity or else infinite stresses will be encountered, and from (40) the sign of $x_1'$ must agree with that of $\cos\psi$.

*Sector Limits.* The vertex sector is adjoined by two flat sectors. Therefore, the orientation of the strain vector is restricted to

$$\tan(-\phi^+) \leqslant \frac{\gamma_{31}'}{\gamma_{32}'} \leqslant \tan\phi^-, \tag{42}$$

where $\phi^+$ and $\phi^-$ are defined in Fig. 3 as $\phi^+ = \omega^+ - \psi$ and $\phi^- = \psi - \omega^-$. Thus, using (37), (39) and (41), leads to

$$[\tan\psi - (n+1)\tan(\psi - \omega^+)]/n \geqslant \tan(\theta - \psi) \geqslant [\tan\psi - (n+1)\tan(\psi - \omega^-)]/n. \tag{43}$$

Simplifying (43), it is obtained that the vertex sector starts (or ends) at $\theta = \theta^{V-}$ (or $\theta^{V+}$), given by

$$\tan\theta^V = (n+1)\frac{\tan(\omega - \psi) + \tan\psi}{n - \tan^2\psi - (n+1)\tan\psi\tan(\omega - \psi)} \tag{44}$$

with $\omega = \omega^-$ (or $\omega^+$). It is interesting to note that (34) and (44) yield exactly the same expression if $\tan(\omega - \psi)$ is expanded and the terms are regrouped. This means that there is no overlap or gap between the two types of sector. In other words, the flat sector ends at exactly the same angle that the vertex sector starts and vice-versa. Therefore, either (34) or (44) will define the range of the applicability of each sector, determining all the unknown constants ($C_2$ must remain for normalization with the outer field). Continuity of the stresses and displacements will thus result, when either (34) or (44) is used as the boundary angle, provided that the range of each sector is finite.

## $J$-INTEGRAL NORMALIZATION

As mentioned earlier the constant $C_2$ was left free for matching with the outer field solution. Such normalization is possible through the path-independent $J$-integral, which is the integral $J_1$ of the pair of integrals

$$J_\beta = \int_{-\pi}^{+\pi} \left[ \frac{n}{(n+1)} \tau\gamma e_\beta - e_\alpha \sigma_{\alpha 3} \partial u_3 / \partial x_\beta \right] r \, d\theta, \quad \beta = 1, 2. \tag{45}$$

Here the path for evaluation is taken as a circle of radius $r$. The contribution of each type of sector can be calculated separately by noting that $J_\alpha$ is a vector subject to the transformation rule of (2). Therefore, $J'_\alpha$ can be evaluated in the rotated coordinate system for that sector resulting in elementary integrals. Then, the contribution from that sector to $J = J_1$ can be calculated directly. The results of these calculations are

$$J_1^F = \left[ -\frac{C_2}{n} \sin^2 \omega \cot(\theta - \omega) \right]_{\theta^{F-}}^{\theta^{F+}}, \tag{46}$$

for the flat sector, and for the vertex sector

$$J_1^V = [nC_2 \cos^2 \psi \tan(\theta - \psi)]_{\theta^{V-}}^{\theta^{V+}}. \tag{47}$$

## APPLICATION TO ISOTROPIC MATERIAL

It is noted here that the present formulation reproduces the known singular field for isotropic materials in mode III. In this case the yield surface is a circle in the space of the ratios of stress to the effective stress $\tau$. A circle can be taken as the limit of an infinitely-sided polygon. Therefore, the general solution presented here does apply to this case. There are two possible approaches to the limit process. First, a point on the circle could be taken to correspond to the limit of the vertex sector. Then, (35) to (44) will apply with the substitution $\alpha = 1$. However, since the cone of the limiting normals vanishes to a single vector at the limit, the direction of the strain vector, which is normal to the circle, is fixed. Using the coordinate system used in the vertex sector leads to $\gamma'_{31} = 0$. Thus from (39) and (41), the angle $\psi$ which determines the location on the yield surface is obtained from

$$\tan(\theta - \psi) = \frac{1}{n} \tan \psi. \tag{48}$$

Using (48) and the transformation rule (2), and normalizing the results with the $J$-integral, the complete solution for mode III cracks in isotropic material is obtained as

$$J = C_2 \frac{(n+1)^2}{n} \frac{\pi}{2},$$

$$u = \gamma r(n+1) \sin \psi / \sqrt{n^2 \cos^2 \psi + \sin^2 \psi},$$

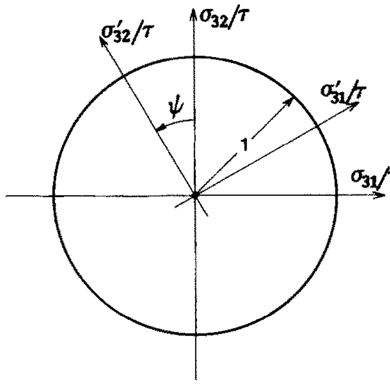


FIG. 4. Yield surface for isotropic material under mode III loading.

$$\gamma = a^{1/(n+1)} \left[ \frac{2J}{\pi r(n+1)} \sqrt{n^2 \cos^2 \psi + \sin^2 \psi} \right]^{n/(n+1)},$$

$$\tau = (\gamma/a)^{1/n},$$

$$\sigma_{31} = -\tau \sin \psi, \ \sigma_{32} = \tau \cos \psi,$$

$$\gamma_{3\alpha} = \gamma \sigma_{3\alpha}/\tau. \tag{49}$$

Exactly the same results are obtained if a point on the circle is taken to correspond to the limit of an infinitesimally small flat sector. Then, using (23) to (34), and observing that at this point the direction of principal shear stress and strain are the same, one sets $\sigma'_{31} = 0$.

The angle $\psi$ in (48) is the angle of principal shear stress (or strain) with the vertical as shown in Fig. 4. It corresponds exactly to angle $\phi$ in RICE (1968, p. 257; 1967, p. 295). These results in fact are exactly the same as RICE's asymptotic solution.

HULT and MCCLINTOCK (1956) derived the complete elastic–ideally plastic crack solution for an isotropic material under anti-plane shear loading. Their result indicated that for small-scale yielding the plastic zone is confined to a circle at the tip of the crack and that $\gamma_{3\theta}$ is proportional to $\cos\theta/r$, while for large scale yielding the plastic zone is elongated in the direction of the crack, and $\gamma_{3\theta}$ has still a $1/r$ singularity. RICE (1967) expanded their result to include general types of hardening, including the power-law hardening material. He found that for small-scale yielding the plastic zone is still a circle, although its center moves closer to the crack tip as the power-law hardening exponent $n$ is decreased. His solution as just rederived yields the HULT and MCCLINTOCK small-scale yielding solution exactly in the limit of $n \to \infty$ everywhere within the plastic zone. For large scale yielding RICE found that the HRR type field is the first term in an infinite series defining the strain and that it dominated the field sufficiently near the tip, within the plastic zone, only for finite $n$. But as $n$ approached the perfectly plastic limit, the actual strain field arbitrarily near the tip deviated from the HRR solution. In that limit, although the strain still has a $1/r$ singularity, the $\theta$

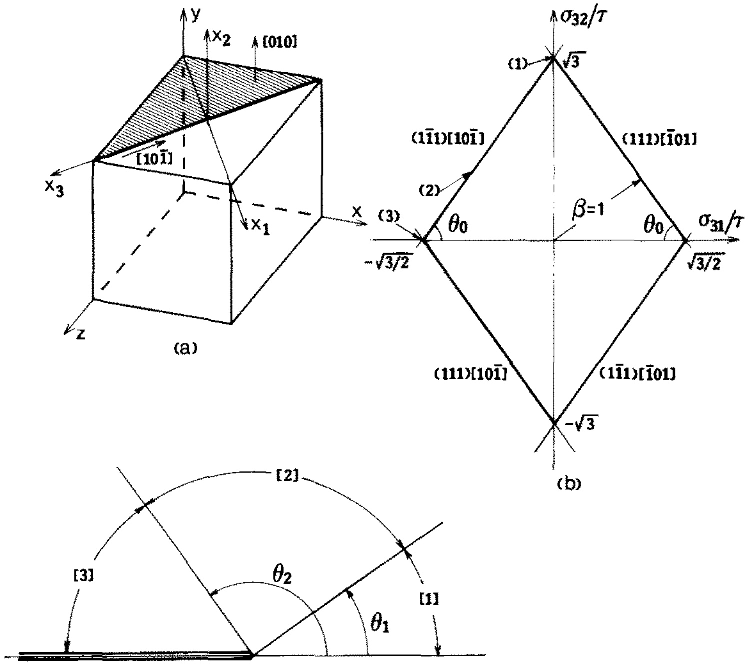


FIG. 5. (a) Fcc or bcc crystal with crack on (010) plane and its tip along [10$\bar{1}$] direction; (b) yield surface for the fcc crystal in this orientation, same result applies to bcc crystal except that the labelling of the normals and directions for the associated slip systems should be interchanged; (c) assumed sector arrangement for this orientation; the numbers refer to (b).

dependence is different, since every term in the series has a singularity of the same order and the HRR solution is no longer the dominant term.

For mode I, as was shown by RICE (1968), even for small-scale yielding the HRR field does not describe the entire plastic zone, and is dominant only immediately adjacent to the crack tip. As the distance from the tip is increased, the actual strain field starts to deviate from the HRR solution.

It is later argued that the HRR fields derived here for cracks in crystals cannot apply throughout the plastic region, even for small scale yielding, but rather dominate the field sufficiently close to the crack for finite $n$. Further, by comparison to the exact ideally plastic solutions for cracked crystals by RICE and NIKOLIC (1985), it is explained that the region of dominance at least of the HRR strain field must shrink to zero as $n \to \infty$.

## CRACKS ON $\{010\}$ CUBE FACE PLANES IN FCC AND BCC CRYSTALS

As a first pair of examples, cracks on the (010) cube-face planes of fcc and bcc crystals, with their tips along the face-diagonal directions [10$\bar{1}$] are analyzed. The crack and crystal orientation are shown in Fig. 5(a). For the fcc crystal, there are twelve different possible slip systems, consisting of the four $\{111\}$ slip planes with three $\langle 110\rangle$ slip directions on each system. The resulting yield surface, which is the inner envelope of all the lines of critical shear, for all possible systems, in the two dimensional anti-plane shear stress space is shown in Fig. 5(b). Active members of the $\{111\}\langle 110\rangle$ type systems are marked along each such line.

For bcc crystals with cracks of this orientation, the primary slip systems are of $\{110\}\langle 111\rangle$ type. Systems of $\{211\}\langle 111\rangle$ type can also flow in bcc metals, but if it is assumed that they have the same critical shear strength, only the $\{110\}\langle 111\rangle$ system will yield in the present case. Thus each pair of vectors giving **n** and **s** for a fcc slip system gives **s** and **n**, respectively, for a bcc slip system and conversely. Since the present "small strain" formulation neglects the finite rotation of the crystal lattice relative to the material, the formulation is invariant to interchange of **n** and **s**. Hence the yield surface for the bcc case is identical to that in Fig. 5(b), except the labelling of slip planes and slip directions for each flat segment should be interchanged. It follows that the solution for the stress and strain fields are identical for the fcc and bcc cases. This is so even though the former involves activation of slip planes that contain the $x_3$ direction and the latter slip planes that are perpendicular to that direction. Implications for the very different patterns of dislocation generation and motion necessary to accomplish the macroscopically identical flow fields in the two cases are discussed by Rice and Nikolic (1985).

The angle $\theta_0$ in Fig. 5(b) is given by $\theta_0 = \arctan(\sqrt{2}) = 54.74°$. However, $\theta_0$ has been left as an unspecified parameter in what follows so that the analysis applies to some other cases as well. For example, the yield surface with $\theta_0 = 45°$ (but with $\beta$ of Fig. 2 equal to $\sqrt{3}$ rather than 1) describes the case of fcc crystal with crack on the (010) cube face but tip along [001] face edge. The normalized yield surface for that case is shown by Rice and Nikolic (1985, Fig. 8) and, for example, the line segment analogous to that along which the numbering (1), (2), (3) appears in Fig. 5(b) then involves simultaneous equal shearing on the $(111)[\bar{1}10]$ and $(\bar{1}\bar{1}1)[\bar{1}10]$ systems.

On the crack surfaces the stress $\sigma_{32} = 0$. For a positive anti-plane shear loading, $\sigma_{31}$ is positive on the lower surface of the crack and negative on the upper surface. Thus, for example, a point on the upper surface of the crack should correspond to the intersection of the flat segment marked (2), in Fig. 5(b), with the $\sigma_{31}/\tau$ axis. Due to symmetry of the yield surface about the $\sigma_{32}/\tau$ axis, the field should also be symmetric about $\theta = 0$ along which ray $\sigma_{31} = 0$. Thus, traversing counter-clockwise around the crack from $\theta = 0$ to $\theta = \pi$ corresponds to going counter-clockwise on the yield surface from point (1) to point (3) of Fig. 5(b) along line (2). The assumed arrangement of angular sectors corresponding to these two vertices and flat segment stress states is shown in Fig. 5(c), where the corresponding regions are numbered and their boundary angles $\theta_1$, $\theta_2$ are to be determined. The values of $\alpha$, $\omega$, and $\psi$ necessary for determining the constants of the previous sections can be readily calculated with simple geometry. Then, using either (34) or (44), the limits of each sector are calculated as

$$\tan\theta_1 = \left(\frac{n+1}{n}\right)\tan\theta_0, \quad \text{with} \quad \theta_1 = \theta_0 \text{ for } n \to \infty,$$
$$\theta_2 = \pi. \tag{50}$$

That is, a finite angular sector [3] does not exist and the stress field with sector [2] should end at point (3) of the yield surface. This means that there is no region of double slip adjoining the crack surfaces. Using (46) and (47), the contribution of each sector to the $J$-integral can be evaluated and added to obtain

$$J = 2C_2 \frac{(n+1)^2}{n} \tan\theta_0. \tag{51}$$

Substituting the value for $C_2$ from (51) into (30) and (40) the equations governing each region become

*Sector* [1], $0 \leqslant \theta \leqslant \arctan\left[\left(\frac{n+1}{n}\right)\tan\theta_0\right]$:

$$\begin{aligned}
&u = \gamma r \cos\theta_0 \sin\theta/\beta,\\
&\gamma = a^{1/(n+1)}\left[\frac{Jn\cot\theta_0}{2r(n+1)\cos\theta}\right]^{n/(n+1)},\\
&\gamma_{31} = -\frac{\gamma n}{\beta(n+1)}\cos\theta_0\tan\theta, \qquad \gamma_{32} = \gamma\cos\theta_0/\beta,\\
&\sigma_{31} = 0, \qquad \sigma_{32} = \tau\beta/\cos\theta_0.
\end{aligned} \tag{52}$$

*Sector* [2], $\arctan\left[\left(\frac{n+1}{n}\right)\tan\theta_0\right] \leqslant \theta \leqslant \pi$:

$$\begin{aligned}
&u = (n+1)\gamma r \sin(\theta-\theta_0)/\beta,\\
&\gamma = a^{1/(n+1)}\left[\frac{J\cos\theta_0}{2r(n+1)\sin(\theta-\theta_0)}\right]^{n/(n+1)},\\
&\sigma_{31} = \frac{\tau\beta}{(n+1)}\left[\frac{\cos\theta}{\sin(\theta-\theta_0)} - \frac{n}{\sin\theta_0}\right],\\
&\sigma_{32} = \frac{\tau\beta}{(n+1)}\frac{\sin\theta}{\sin(\theta-\theta_0)},\\
&\gamma_{31} = -\gamma\sin\theta_0/\beta, \quad \gamma_{32} = \gamma\cos\theta_0/\beta
\end{aligned} \tag{53}$$

where, again, $\beta = 1$ and $\theta_0 = 54.74^\circ$ for the fcc and bcc cases of Fig. 5. Also, $\tau$ is given by (10) as $\tau = (\gamma/a)^{1/n}$. The stress distributions are plotted in Fig. 6 and the strain distributions in Fig. 7 for various values of $n$. Also, Fig. 8 shows the resulting triangular form of the contour of constant equivalent strain $\gamma$ (and hence also a contour of constant slip system strength $\tau$), as well as the contour of constant shear strain from a single one of the two slip systems active simultaneously in sector [1]. Note that if these systems are labelled "1" and "2", corresponding to the flat segments to the left and right of uppermost vertex, labelled (1) in Fig. 5(b), then from (2),

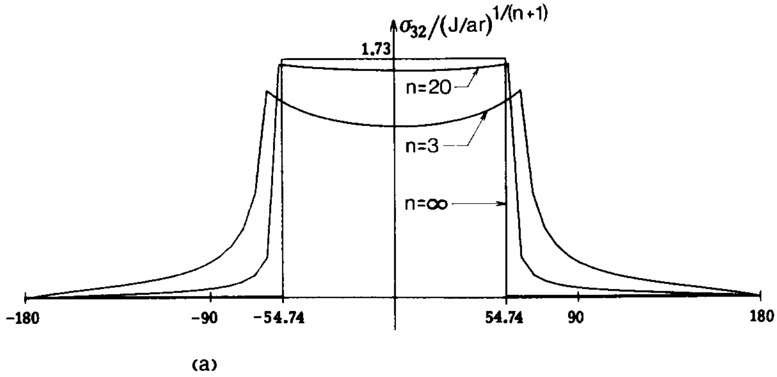


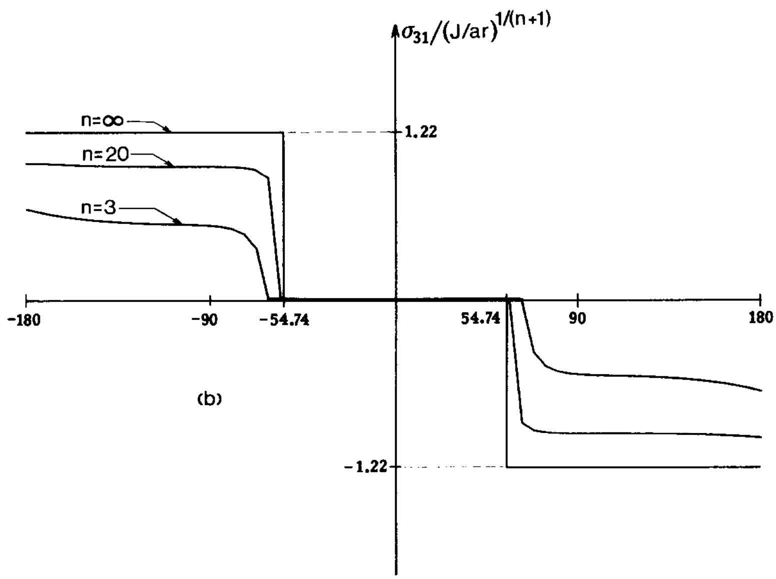


FIG. 6. Fcc or bcc crystal with crack on (010) plane and its tip along [10$\bar{1}$] direction; (a) the stress $\sigma_{32}$; (b) the stress $\sigma_{31}$; both for various $n$.

$\gamma_{32} = (\gamma^2+\gamma^1)\cos\theta_0$ and $\gamma_{31} = (\gamma^2-\gamma^1)\sin\theta_0$ where $\gamma^1$ and $\gamma^2$, summing to $\gamma$, are the respective shear strains. This enables the calculation of $\gamma^1$ and $\gamma^2$ from (52).

Note that for the ideally plastic limit $n \to \infty$, the above results reduce to

*Sector* [1]:

$$u = [J/(2\tau_0\beta)]\cos\theta_0\cot\theta_0\tan\theta,$$

$$\gamma = [J/(2r\tau_0)]\cot\theta_0\sec\theta,$$

$$\gamma_{31} = -\gamma\cos\theta_0\tan\theta/\beta, \qquad \gamma_{32} = \gamma\cos\theta_0/\beta,$$

$$\sigma_{31} = 0, \qquad \sigma_{32} = \tau_0\beta/\cos\theta_0. \tag{54}$$

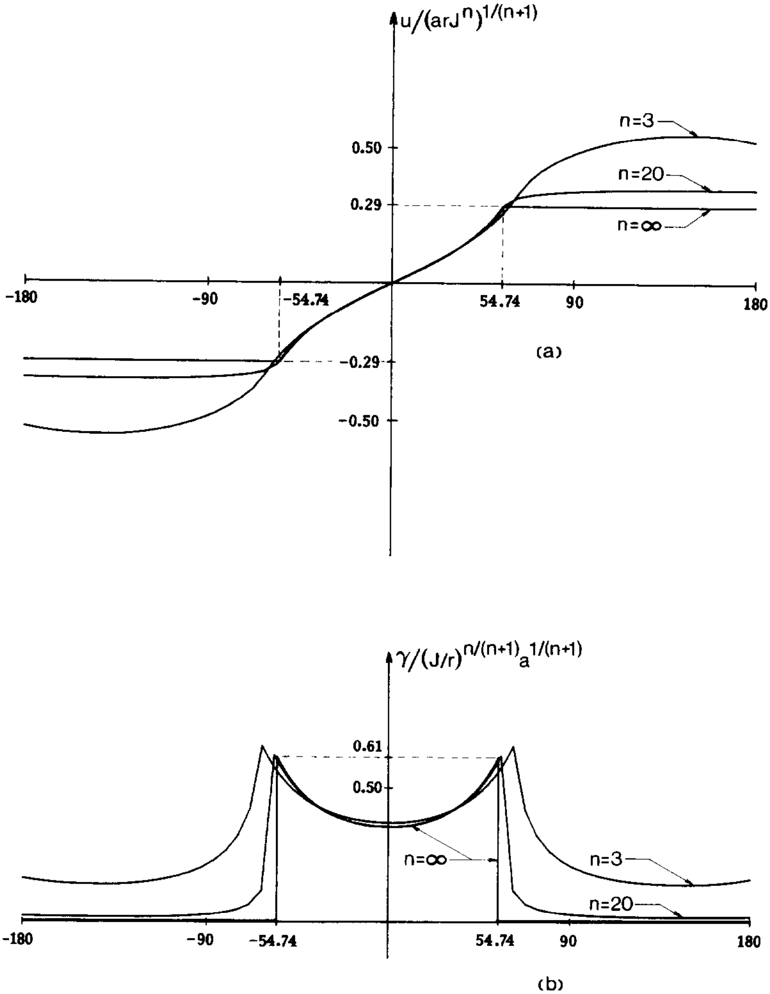


FIG. 7. Fcc or bcc crystal with crack on (010) plane and its tip along [10$\bar{1}$] direction; (a) displacement $u$; (b) the equivalent shear strain $\gamma$, both for various values of $n$.

*Sector* [2]:

$$u = [J/(2\tau_0\beta)]\cos\theta_0,$$

$$\gamma = \gamma_{31} = \gamma_{32} = 0,$$

$$\sigma_{31} = -\tau_0\beta/\sin\theta_0, \quad \sigma_{32} = 0, \tag{55}$$

where $\tau_0$ is the yield stress in shear. Although the stress field shows exactly the same discontinuity as RICE and NIKOLIC (1985), that is, it is constant in each sector with jumps on the sector boundaries, the displacement field is completely continuous and the strain $\gamma$ is non-zero throughout sector [1]. By contrast the complete RICE and NIKOLIC elastic–plastic solution involves plastic flow on discrete planes of dis-

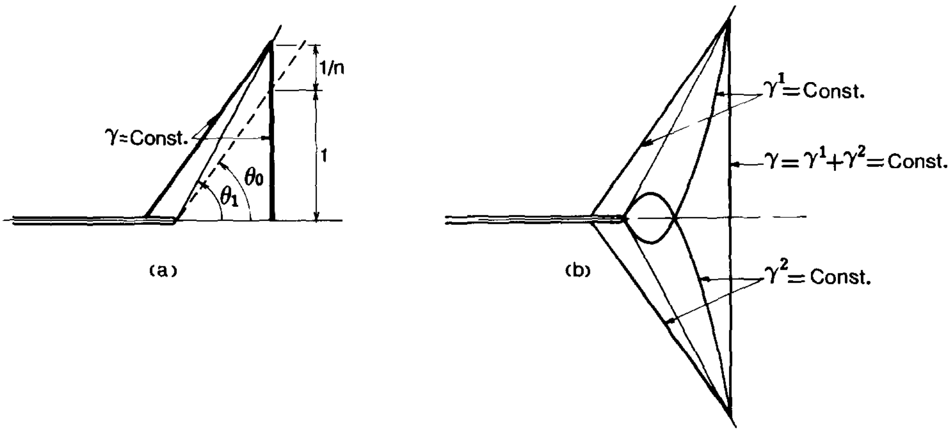


FIG. 8. Fcc or bcc crystal with crack on (010) plane and its tip along [10$\bar{1}$] direction; (a) contour of constant strain $\gamma$, which is triangular for all $n$; (b) contour of constant strain $\gamma^1$ associated with a single flat segment meeting at a vertex, both drawn for $n = 3$.

continuity emanating from the tip at the sector boundary, across which both stress and displacement are discontinuous. Here it should be noted that the field equations for strain in the asymptotic analysis of RICE and NIKOLIC determine stress but allow a family of solutions for the strain. The limit of the HRR field given here is a member (but of the rigid–plastic version) as also, of course, is the complete solution they derived. Therefore, it is inferred that for finite $n$, the HRR field must be the dominant term for only part of the plastic zone even for small-scale yielding (in contrast to the isotropic case), and evidently as $n \to \infty$ the domain of validity of the HRR strain field must shrink to zero. It should be noted that RICE and NIKOLIC obtained displacement $u = 0.346J/\tau_0$ in sector [2], at least for small scale yielding, whereas the limiting HRR result of (55) is $u = 0.289J/\tau_0$.

## FFC CRYSTAL WITH CRACK ALONG A {111} SLIP PLANE

The case studied here is that of the crack on the (111) plane and its tip along the [10$\bar{1}$] direction. The crack configuration is shown in Fig. 9(a), with the corresponding yield surface shown in Fig. 9(b). The assumed sector arrangement is shown in Fig. 9(c) where the numbers refer to regions shown in Fig. 9(b). Here $\beta = 1$ and again, the values of $\alpha$, $\omega$, and $\psi$ can be readily calculated with simple geometry. Then, using either (34) or (44), the limits of each sector are calculated as

$$\begin{aligned} \tan\theta_1 &= -2\sqrt{2}\left(\frac{n+1}{n-2}\right), \quad \text{with} \quad \theta_1 = -70.529^\circ \text{ for } n \to \infty, \\ \theta_2 &= \theta_3 = 0, \\ \tan\theta_4 &= -2\sqrt{2}\left(\frac{n+1}{n+4}\right), \quad \text{with} \quad \theta_4 = 109.471^\circ \text{ for } n \to \infty. \end{aligned} \tag{56}$$

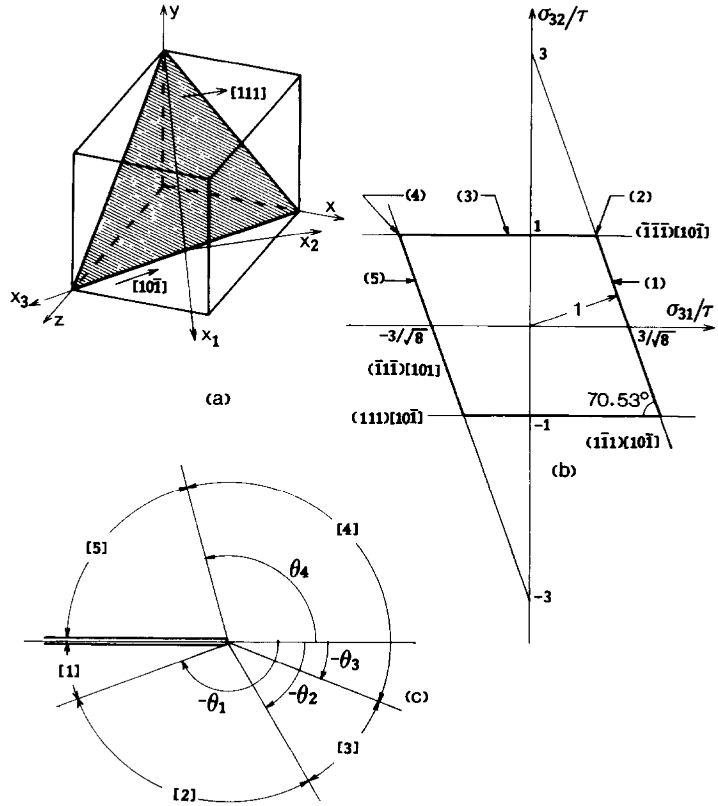


FIG. 9. (a) Fcc crystal with crack on (111) plane and its tip along [10$\bar{1}$] direction; (b) yield surface for this orientation; (c) assumed sector arrangement for this orientation; the numbers refer to (b).

Note that sector [3] collapses to a line along the $x_1$ axis, since $\omega_3 = 0$. Using (46) and (47), the contribution of each sector to the $J$-integral can be evaluated and added to obtain

$$J = \frac{4\sqrt{2}}{3} C_2 \frac{(n+1)^2}{n}. \tag{57}$$

Substituting the value for $C_2$ from (57) into (30) and (40) the equations governing each region become

*Sector* [1], $\quad -\pi \leqslant \theta \leqslant \arctan\left[-2\sqrt{2}\left(\dfrac{n+1}{n-2}\right)\right], \qquad \omega_1 = -70.529°:$

$$u = (n+1)\gamma r \sin(\omega_1 - \theta),$$

$$\gamma = a^{1/(n+1)}\left[\frac{J}{2r(n+1)\sin(\omega_1-\theta)}\right]^{n/(n+1)},$$

$$\sigma_{31} = \frac{\tau}{(n+1)}\left[\frac{\cos\theta}{\sin(\theta-\omega_1)} + \frac{3n}{2\sqrt{2}}\right],$$

$$\sigma_{32} = \frac{\tau}{(n+1)}\frac{\sin\theta}{\sin(\theta-\omega_1)},$$

$$\gamma_{31} = 2\sqrt{2}\gamma/3, \qquad \gamma_{32} = \gamma/3. \tag{58}$$

*Sector* [2], $\arctan\left[-2\sqrt{2}\left(\frac{n+1}{n-2}\right)\right] \leqslant \theta \leqslant 0$, $\psi_2 = -35.264°$:

$$u = \gamma r \sin\theta,$$

$$\gamma = a^{1/(n+1)}\left[\frac{\sqrt{3}Jn}{4r(n+1)\cos(\theta-\psi_2)}\right]^{n/(n+1)},$$

$$\gamma_{31} = -\frac{\gamma n\sqrt{2}}{(n+1)\sqrt{3}}\frac{\sin\theta}{\cos(\theta-\psi_2)},$$

$$\gamma_{32} = \frac{\gamma}{(n+1)}\left[\sqrt{(2/3)}\, n\frac{\cos\theta}{\cos(\theta-\psi_2)} + 1\right],$$

$$\sigma_{31} = \tau/\sqrt{2}, \quad \sigma_{32} = \tau. \tag{59}$$

*Sector* [4], $0 \leqslant \theta \leqslant \arctan\left[-2\sqrt{2}\left(\frac{n+1}{n+4}\right)\right]$, $\psi_4 = 54.736°$:

$$u = \gamma r \sin\theta,$$

$$\gamma = a^{1/(n+1)}\left[\frac{\sqrt{3}Jn}{4\sqrt{2}r(n+1)\cos(\theta-\psi_4)}\right]^{n/(n+1)},$$

$$\gamma_{31} = -\frac{\gamma n}{(n+1)\sqrt{3}}\frac{\sin\theta}{\cos(\theta-\psi_4)},$$

$$\gamma_{32} = \frac{\gamma}{(n+1)}\left[(n/\sqrt{3})\frac{\cos\theta}{\cos(\theta-\psi_4)} + 1\right],$$

$$\sigma_{31} = -\tau\sqrt{2}, \qquad \sigma_{32} = \tau. \tag{60}$$

*Sector* [5], $\arctan\left[-2\sqrt{2}\left(\frac{n+1}{n+4}\right)\right] \leqslant \theta \leqslant \pi$, $\omega_5 = 109.471°$:

$$u = (n+1)\gamma r \sin(\theta-\omega_5),$$

$$\gamma = a^{1/(n+1)}\left[\frac{J}{2r(n+1)\sin(\theta-\omega_5)}\right]^{n/(n+1)},$$

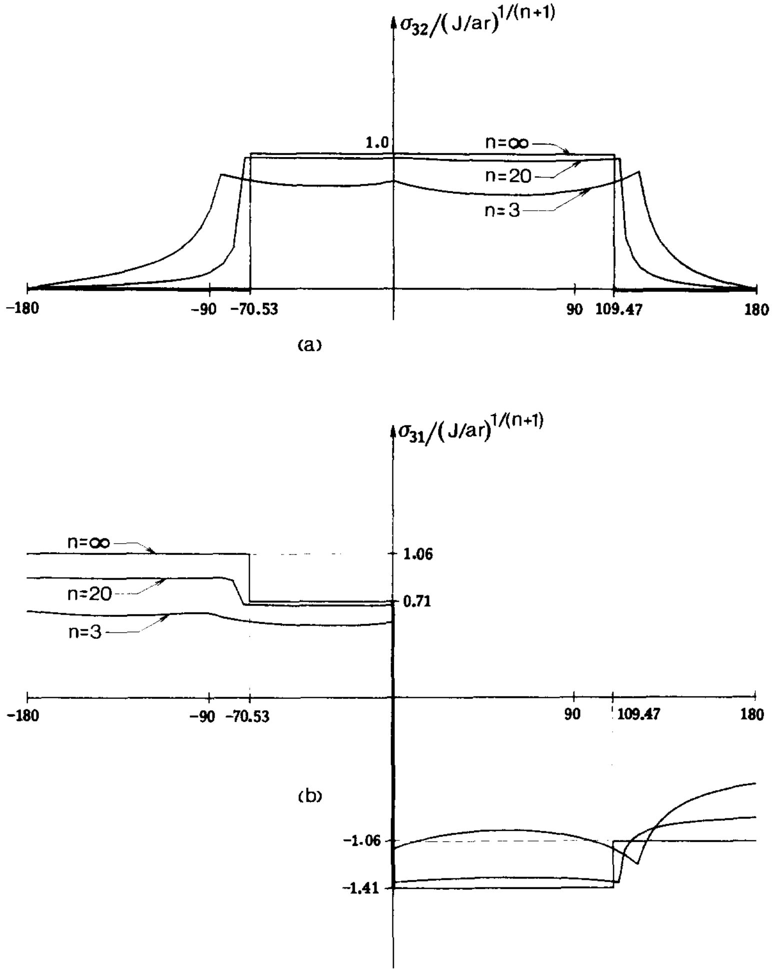


FIG. 10. Fcc crystal with crack on (111) plane and its tip along $[10\bar{1}]$ direction; (a) the stress $\sigma_{32}$; (b) the stress $\sigma_{31}$; both for various values of $n$.

$$\sigma_{31} = \frac{\tau}{(n+1)}\left[\frac{\cos\theta}{\sin(\theta-\omega_5)} - \frac{3n}{2\sqrt{2}}\right],$$

$$\sigma_{32} = \frac{\tau}{(n+1)}\frac{\sin\theta}{\sin(\theta-\omega_5)},$$

$$\gamma_{31} = -2\sqrt{2}\gamma/3, \qquad \gamma_{32} = -\gamma/3. \tag{61}$$

In the above equations again, $\tau$ is given by (10) as $\tau = (\gamma/a)^{1/n}$. The graphs of the stress and strain distributions are shown in Figs 10 and 11 for various values of $n$, with the contour of constant strain $\gamma$ and the boundary between each region in Fig. 12.

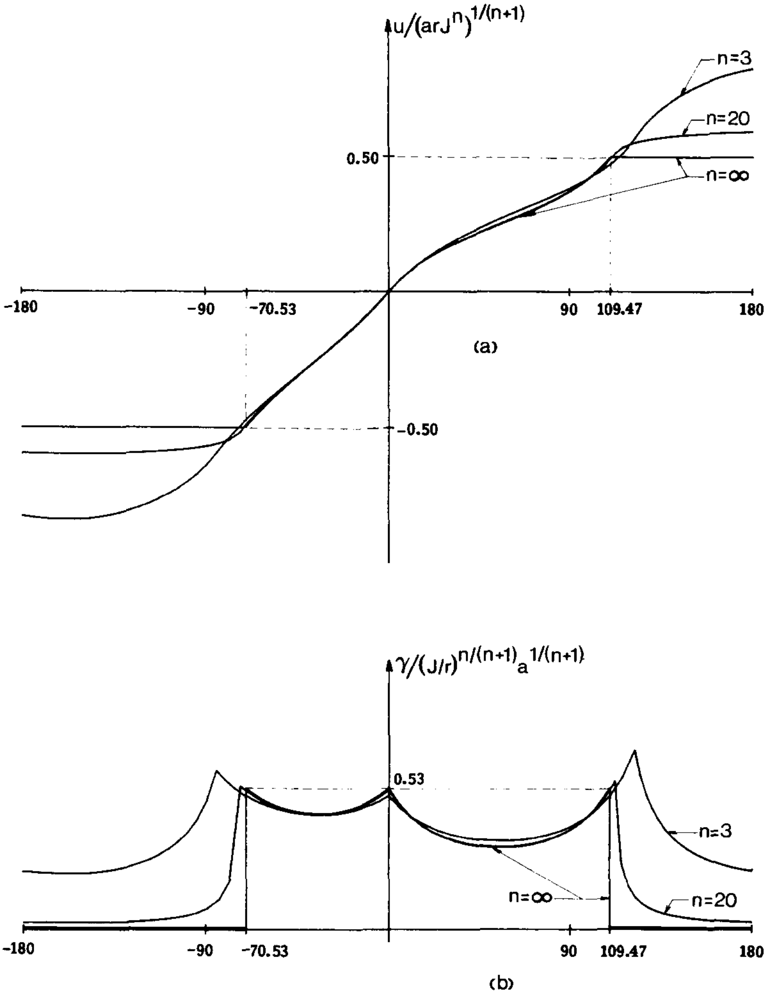


FIG. 11. Fcc crystal with crack on (111) plane and its tip along [10$\bar{1}$] direction; (a) displacement $u$; (b) the equivalent shear strain $\gamma$, both for various values of $n$.

Note that associated with the collapsing of sector [3] there is a discontinuity in the stress $\sigma_{31}$ (or more appropriately $\sigma_{3r}$) at $\theta = 0$, while all other stresses and displacements remain continuous. For the entirely plastic constitutive response which determines the near-tip singularity, such a discontinuity in stress, from vertex (2) to (4) in Fig. 9(b), need cause no discontinuity in strain.

To illustrate the nature of this discontinuity more clearly, another example has been solved, for which the crack is rotated off the (111) plane, but still has its tip along [10$\bar{1}$], as in Fig. 13(a). The yield surface rotates a corresponding amount $\phi$ around the origin as shown in Fig. 13(b), with a sector arrangement shown in Fig. 13(c). As the angle $\phi$ varies from zero to $\theta_0 = 54.736°$, the result varies from that of

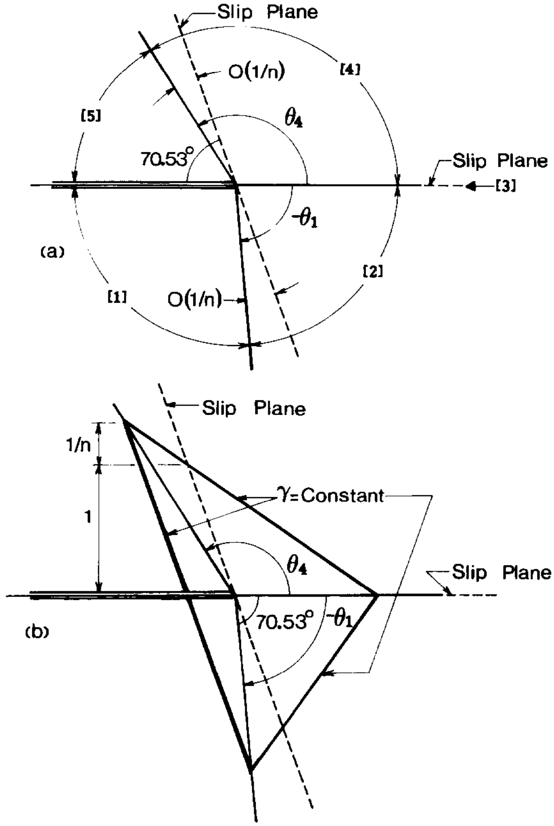


FIG. 12. Fcc crystal with crack on (111) plane and its tip along $[10\bar{1}]$ direction; (a) boundary of the different regions, with the slip planes shown as dashed lines, drawn for $n = 3$; (b) contour of constant strain $\gamma$, which is triangular for all $n$.

Figs 5 to 8, the fully symmetric solution, to that of Figs 9 to 12, the discontinuous solution. For a general $\phi$ it is obtained from (34) or (44) that

$$\tan\theta_1 = -(n+1)\frac{\cot\phi+\cot\theta_0}{n-\cot^2\phi-(n+1)\cot\phi\cot\theta_0},$$

$$\tan\theta_2 = -(n+1)\frac{\cot\phi-\cot\theta_0}{n-\cot^2\phi+(n+1)\cot\phi\cot\theta_0},$$

$$\tan\theta_3 = -(n+1)\frac{\tan\theta_0-\tan\phi}{n-\tan^2\phi+(n+1)\tan\phi\tan\theta_0},$$

$$\tan\theta_4 = +(n+1)\frac{\tan\theta_0+\tan\phi}{n-\tan^2\phi-(n+1)\tan\phi\tan\theta_0}. \tag{62}$$

Figure 14 shows the stress $\sigma_{31}/\tau$ plotted for various values of $\phi$, while Fig. 15 enlarges the zone of rapid variation. Note that the results approach the discontinuous solution

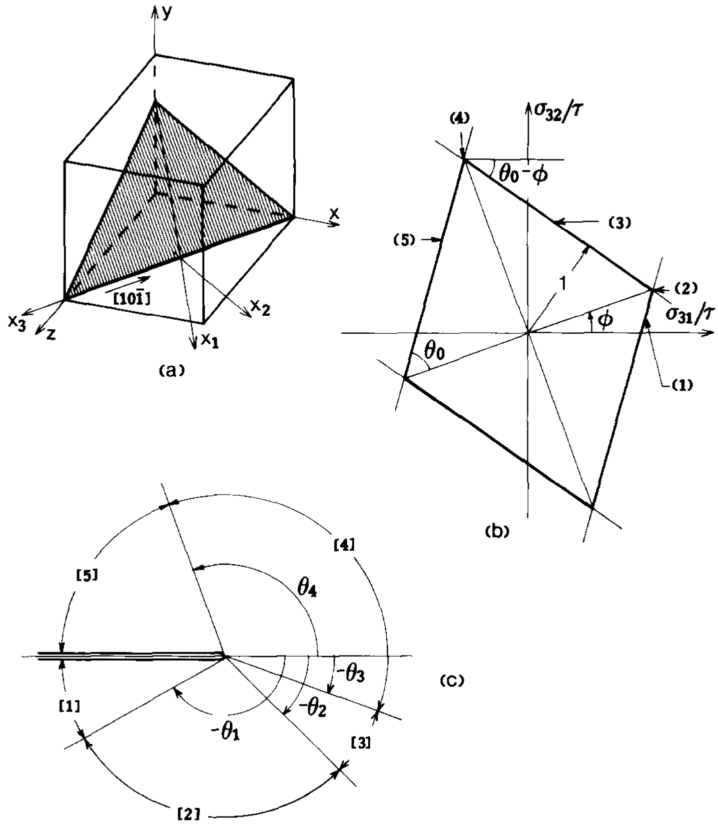


FIG. 13. (a) Fcc crystal with crack tip along [10$\bar{1}$] direction, and crack plane being any plane for which [10$\bar{1}$] is the zone-axis; (b) yield surface for this orientation; (c) assumed sector arrangement for this orientation; the numbers refer to (b).

very rapidly. For example, region [3] encompasses only a range of 1.43° for $\phi = 45°$. Denoting $\theta_0 - \phi = \lambda$, as $\lambda \to 0$, it is observed that region [3] vanishes as,

$$\theta_3 - \theta_2 = \frac{2}{\sin 2\theta_0} \frac{(n+1)}{n^2} \lambda^2. \tag{63}$$

That is, the stresses are continuous as $\phi \to \theta_0$, yet they drop very rapidly over a very small range. The range becomes even smaller as the value of $n$ increases. In fact, the stress distribution is always discontinuous for the perfectly plastic limit ($n \to \infty$), in which

$$\theta_2 = \theta_3 = \phi - \theta_0. \tag{64}$$

Again observe that as in the previous section, the stress field is exactly the same as RICE and NIKOLIC (1985, p. 606), yet the limiting HRR displacement distribution is continuous and $\gamma$ is non-zero in sectors [2] and [4]. This differs from the complete elastic–plastic solution of RICE and NIKOLIC where again the displacement and stress

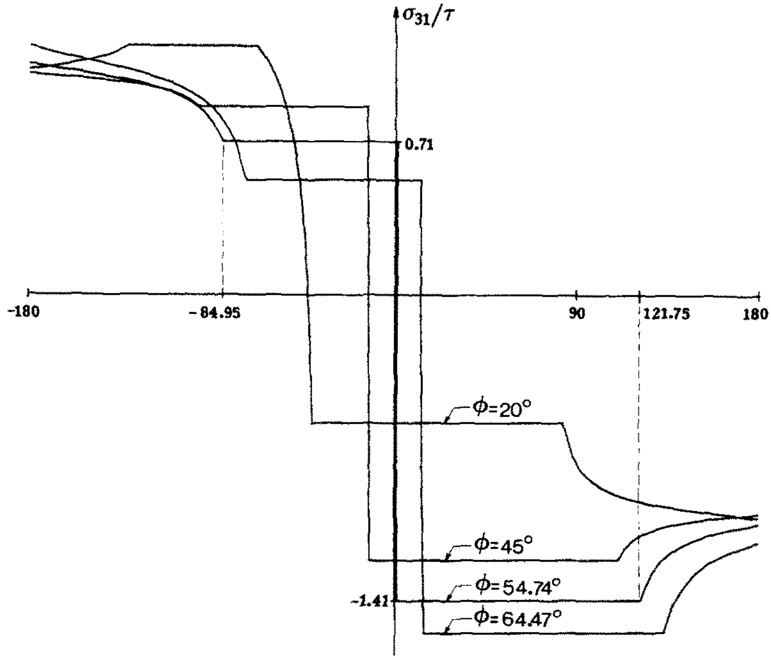


FIG. 14. Fcc crystal with crack tip along [10$\bar{1}$] direction, and crack plane being any plane for which [10$\bar{1}$] is the zone-axis. The stress ratio $\sigma_{31}/\tau$ for various values of $\phi$ and $n = 3$; rapid continuous variation when $\phi \neq 54.74°$, discontinuous variation when $\phi = 54.74°$.

discontinuity occurred over the discrete planes which confined the plastic flow and were parallel to slip planes.

## DISCUSSION

As has been mentioned, it is conjectured that the domain of dominance of the HRR field for single crystals under mode III loading is limited only to a part of the plastic zone which is immediately adjacent to the crack tip. As the perfectly plastic limit is approached, this domain must shrink to zero since the HRR solution does not yield the known perfectly plastic displacement and strain results of RICE and NIKOLIC (1985). The HRR singular field presented here shows a continuous displacement field and finite plastic angular sectors, while the solution of RICE and NIKOLIC shows plastic zones which are discrete planes emanating from the crack tip across which displacement and stress discontinuity occur. These planes lie parallel to the flat segments along the yield surface (in the region $\sigma_{23} > 0$) and in some cases, like those of the fcc case in Fig. 5, and Figs 9 and 13 here, coincide with the crystal slip planes emanating from the tip.

For single crystals the HRR field contours of constant shear strength and equivalent shear strain are triangular as is shown in Figs 8(a) and 12(b). Another possibly observable feature for the single crystal case is that the boundary planes between

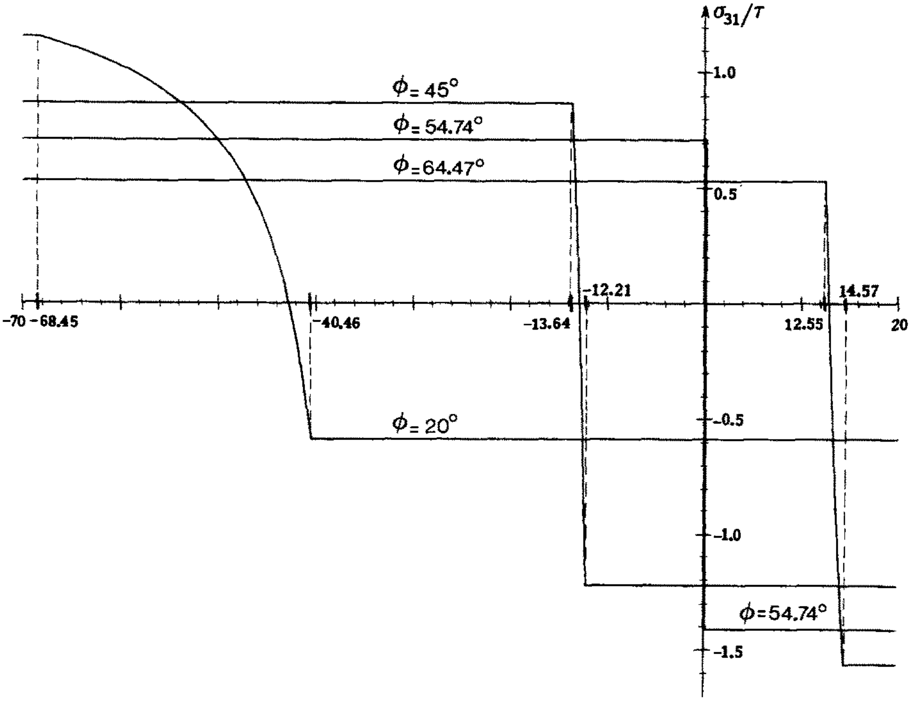


FIG. 15. Fcc crystal with crack tip along [10$\bar{1}$] direction, and crack plane being any plane for which [10$\bar{1}$] is the zone-axis. The rapid variation zone of Fig. 14 enlarged.

regions of single slip (the flat sectors) and double slip (the vertex sectors) differ from planes parallel to the yield surface flat segments (i.e., from the slip planes in cases just noted) by an angle of order $1/n$ for large $n$.

The analysis of the HRR fields in this case has been greatly simplified by the general integral of such fields given by (18), which reduces to (20) for mode III.

## ACKNOWLEDGEMENT

This study was supported by the Office of Naval Research under contract N00014-85-K-0405 with Harvard University.

## REFERENCES

HULT, J. A. and MCCLINTOCK, F. A. 1956 *Proc. 9th Int. Congr. Appl. Mech., Brussels*, **8**, 51–58.
HUTCHINSON, J. W. 1968 *J. Mech. Phys. Solids* **16**, 13–31.
RICE, J. R. 1967 *J. appl. Mech.* **34**, 287–298.
RICE, J. R. 1968 *Fracture, An Advanced Treatise*, Vol. 2 (edited by LIEBOWITZ, H.), Academic Press Inc., New York, pp. 191–311.

Rice, J. R. 1988 "Two General Integrals of Singular Crack Tip Deformation Fields", *J. Elasticity*, to be published.
Rice, J. R. and Rosengren, G. F. 1968 *J. Mech. Phys. Solids* **16,** 1–12.
Rice, J. R. and Nikolic, R. 1985 *J. Mech. Phys. Solids* **33,** 595–622.